

Electron-beam-induced-current study of defects in GaN; experiments and simulation

This article has been downloaded from IOPscience. Please scroll down to see the full text article.

2002 J. Phys.: Condens. Matter 14 13069

(<http://iopscience.iop.org/0953-8984/14/48/352>)

View [the table of contents for this issue](#), or go to the [journal homepage](#) for more

Download details:

IP Address: 171.66.16.97

The article was downloaded on 18/05/2010 at 19:15

Please note that [terms and conditions apply](#).

Electron-beam-induced-current study of defects in GaN; experiments and simulation

E B Yakimov

Institute of Microelectronics Technology, RAS, Chernogolovka 142432, Russia

E-mail: yakimov@ipmt-hpm.ac.ru

Received 27 September 2002

Published 22 November 2002

Online at stacks.iop.org/JPhysCM/14/13069

Abstract

A review is given of the prospects and limitations of the application of the electron-beam-induced-current (EBIC) technique in the study of the extended defects in GaN and related materials. The approaches commonly used for the analyses of the EBIC data are discussed. The profile of the dislocation EBIC contrast in materials with diffusion lengths smaller than the electron range is analysed. The simulation carried out shows that at small enough diffusion length values, the width of the dislocation contrast could decrease with increasing primary electron energy. It is demonstrated that in GaN structures the diffusion length can be estimated from the dislocation profile. The minimum defect cylinder radius which can be extracted from the EBIC measurements is evaluated. A pronounced dependence of threading dislocation EBIC contrast in n-GaN on the beam current is revealed, which could be caused by the dislocation charge.

1. Introduction

The increasing application of group III nitrides in light-emitting diodes, lasers and advanced electronic devices is generating interest in the study of electrical and optical properties of defects in these materials. Group III nitride epilayers usually contain a high density of extended defects such as threading dislocations (edge, mixed and screw), nanopipes, stacking faults and inversion domain boundaries [1]. The dislocation properties of GaN and its alloys are particularly intriguing, because high-performance light-emitting diodes and lasers have been fabricated using GaN despite a density of dislocations (typically in the range from 10^8 to 10^{10} cm⁻²) that is high enough to degrade the device performance in other III–V materials. In spite of widespread effort to reach a consensus, there have been many conflicting views on the role of the threading dislocations in GaN. Earlier studies suggested that dislocations did not act as recombination centres in GaN-related materials [2]. Then, it was shown [3–6] that dislocations act as nonradiative recombination centres, although the devices fail due to other nonradiative recombination defects [7]. Analyses of carrier transport data [8, 9],

differential photoelectrochemical etching [10], studies using a combination of atomic force and scanning capacitance microscopy [11], scanning Kelvin probe microscopy [12] and electron holography studies [13] suggest that dislocations in GaN are negatively charged, while ballistic electron emission microscopy found no indication of fixed negative dislocation charge [14]. The discrepancies in the measured dislocation properties could be caused by the difficulties of separating the intrinsic properties of the dislocation core from the effects of impurities and point defects. There are also notable inconsistencies in the theoretical simulations of intrinsic dislocation properties in GaN. Thus, calculations carried out in [15, 16] did not predict states in the band gap and concluded that the dislocation electrical activity was related to the segregation of dopants, impurities or intrinsic point defects, while in [17, 18] it was shown that dislocation-related energy states in the band gap should be formed.

To understand the properties of dislocations in GaN, methods providing quantitative information about individual defects should be used. One such method uses the electron-beam-induced-current (EBIC) mode of the scanning electron microscope; this has been widely used for the study of individual extended defect recombination properties in semiconductor structures [19, 20]. A model of the extended defect EBIC contrast has been proposed [21, 22], which allows one not only to describe the contrast profile but also to extract the defect recombination strength value from the EBIC measurements. To obtain the recombination defect parameters from the recombination strength, a few approaches based on the measurements of EBIC contrast dependence on temperature and/or excitation level have been proposed [20, 23, 24]. However, the models mentioned were developed for semiconductors with a high enough minority carrier diffusion length. Thus, the question arises of the applicability of these approaches to materials with diffusion lengths much smaller than the electron range that is typical for GaN and related materials.

In the present paper, the recent state of individual defect characterization by the EBIC method is discussed; the applicability of approaches commonly used for the description of defects in GaN-based materials is analysed. The results of EBIC contrast simulation for individual dislocations perpendicular to the surface are presented; the simulated profiles are compared with experimental ones. It is found that at very small diffusion length the EBIC profile width can decrease with increasing primary electron energy. It is shown that in the structures with low diffusion lengths, even rather narrow depletion regions can affect the EBIC contrast. The possibility of estimation of the radius of defect cylinders related to the dislocations from the EBIC measurements is discussed.

2. Characterization of individual defects in the EBIC mode

In the EBIC mode the current collected by the p–n junction or Schottky barrier is detected. Recombination defects present in the semiconductor structure decrease the collected current and such a decrease can be measured as a function of the distance between defect and e-beam position. The results of such measurements are usually described by the defect contrast $C(r) = 1 - I_c(r)/I_{c0}$, where $I_c(r)$ and I_{c0} are the collected current values, measured with the focused e-beam located at point r near the defect and far from it, respectively. As shown in [21, 22], for a small enough contrast the recombination properties of uncharged defects can be characterized by their recombination strength $\gamma_d = V_d(1/\tau_d - 1/\tau_b) \approx V_d/\tau_d$, where V_d is the volume in which the minority carrier recombination is changed; τ_d and τ_b are the minority carrier lifetimes in the defect region and in the bulk, respectively. In this approximation a dislocation can be described as a defect cylinder with radius r_d and lifetime τ_d inside the cylinder; thus, the dislocation recombination strength is

$$\gamma_d = \pi r_d^2(1/\tau_d - 1/\tau_b) \approx \pi r_d^2/\tau_d = N_{tot}\sigma v_{th}, \quad (1)$$

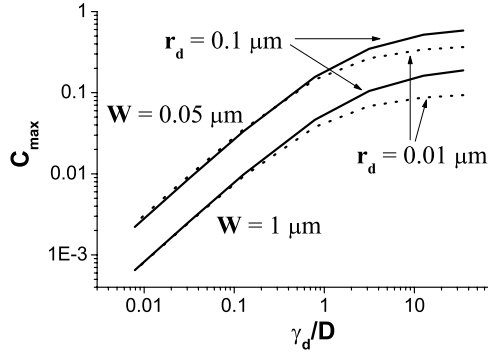


Figure 1. Dependences of C_{max} on γ_d/D for dislocations perpendicular to the surface in Si simulated for a few different values of W and r_d ; $L_b = 50 \mu\text{m}$, $R = 5 \mu\text{m}$.

where N_{tot} is the trap linear density in the dislocation core, σ is their capture cross-section and v_{th} is the thermal velocity of minority carriers. Under such assumptions, in the geometry with the e-beam perpendicular to the Schottky barrier, a dislocation located parallel to the barrier at a depth z_0 and a very small depletion region width W ($W \ll z_0$ and $W \ll R$, where R is the electron range), the maximum of the dislocation EBIC contrast C_{max} can be approximated as [22]

$$C_{max} = \frac{\gamma_d}{1 + \frac{\gamma_d}{2\pi D} [\ln(2z_0/r_d) + 1/2]} \frac{\exp(-z_0/L_b) \int_{-\infty}^{\infty} p_0(0, y, z_0) dy}{I_{c0}} \quad (2)$$

where $p_0(0, y, z_0)$ is the minority carrier concentration at $(0, y, z_0)$ in the sample without dislocations, D is the minority carrier diffusivity and $L_b = \sqrt{D\tau_b}$ is the bulk minority carrier diffusion length. The electron beam intersects the surface in the point $(0, 0, 0)$ and the y -axis is parallel to the dislocation. If W cannot be neglected, equation (2) should be rewritten as

$$C_{max} = \frac{\gamma_d}{1 + \frac{\gamma_d}{2\pi D} [\ln[2(z_0 - W)/r_d] + 1/2]} \frac{\exp[-(z_0 - W)/L_b] \int_{-\infty}^{\infty} p_0(0, y, z_0) dy}{I_{c0}}. \quad (3)$$

It is easy to see that the dependence of C_{max} on γ_d is usually nonlinear and can be considered as linear at small γ_d only. At large enough γ_d the relation between C_{max} and γ_d depends on both z_0 and r_d , i.e. in a common case there is no unequivocal correspondence between these parameters. As seen from (2), (3), the γ_d -range in which the linear approximation can be used is independent of L_b . However, it is not γ_d but the contrast that is measured experimentally and the contrast value could substantially decrease (even at the constant γ_d) with decreasing L_b and increasing W (due to the $p_0(0, y, z_0)$ decrease); therefore small contrast does not guarantee the validity of the linear approximation.

For the dislocations perpendicular to the surface, such as threading dislocations in GaN, the relation between C_{max} and γ_d can be obtained by numerical simulation [25–27]. The results of such simulation for Si with $R = 5 \mu\text{m}$ and $L_b = 50 \mu\text{m}$ are presented in figure 1. It is seen that at W very close to 0 (as was assumed in [22]) the linear approximation can indeed be used up to a contrast value of about 10%, while at $W = 1 \mu\text{m}$ (corresponding to a dopant concentration of about 10^{15}cm^{-3} at zero-bias conditions) such an approximation is valid to a contrast value of only about 1%. For GaN, R is comparable with that for Si (2.6 times smaller) but the dopant concentration is usually much higher; therefore one could assume that the W -effect in this material is insignificant. However, as the simulation has shown, for the small L_b -values it should be taken into account even at $W \ll R$, especially if the dopant

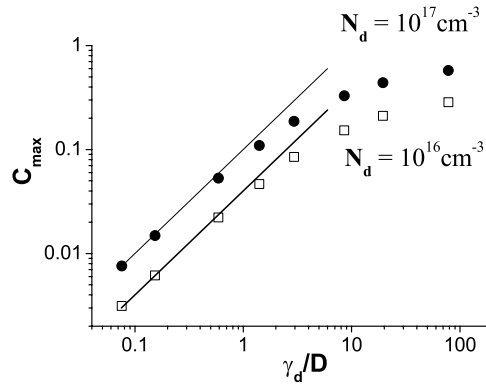


Figure 2. Dependences of C_{max} on γ_d/D for dislocations perpendicular to the surface in GaN calculated with $r_d = 50$ nm, $L_b = 0.2$ μ m, $E_b = 25$ keV.

concentration is not too high (figure 2). The results presented in figure 2 were calculated for GaN keeping r_d constant ($r_d = 50$ nm) and changing τ_d . It is seen that if the contrast is lower than 10%, the linear approximation can be used.

At larger contrast values, the exact relation between C_{max} and γ_d should be calculated and this procedure needs the r_d -value. The knowledge of r_d could also be useful for understanding the defect structure. The r_d -value can be obtained by fitting the EBIC profile or using the procedure based on the measurement of dislocation contrast dependence on bias applied to the collected barrier [26, 27]. As shown in [27], an r_d of about 100–200 nm can be estimated for dislocations in Si using the beam with $R = 5$ μ m by the first method and of about 50 nm by the second one. The width of the dislocation EBIC profile was shown [21] to be determined by the generation function dimensions and to be practically independent of the diffusion length. However, this is true only when L_b is larger than R and the calculations carried out in [26, 27] were made under just such an assumption. The opposite relation usually applies in GaN. In this case, the diffusion length could affect fundamentally the EBIC contrast profile and this effect should be taken into account.

While the EBIC contrast for individual defects can be described rather well, the questions concerning the extraction of quantitative information about the defect properties from the EBIC images, the kind of information which can be obtained from such measurements and the optimum approaches to the solution of this problem have not received final answers yet, even for dislocations in Si. The common procedure for obtaining the dislocation parameters from the EBIC data consists in the analysis of the γ_d -dependence on the temperature and/or beam current. It should be noted that when the contrast depends on the beam current, expressions (2), (3) should be used with a care, because due to the inhomogeneous excitation, different parts of dislocations are in different excitation conditions. Consequently, if τ_d depends on the excitation level, γ_d could change along a dislocation.

For the analyses of γ_d -dependence on the temperature and/or beam current, the Shockley–Read–Hall (SRH) recombination model [28] or a model taking into account the dislocation charge [23] were used. Recently, a model combining the effect of shallow and deep levels in the dislocation core and taking into account the dislocation charge was proposed [24]. The SRH model could be used without any complementary experiments, while for the correct application of charged dislocation models some parameters, such as dislocation-related energy levels, excess carrier concentration under electron beam excitation, capture cross-sections for the minority and majority carriers etc should be known. It should be stressed that the question

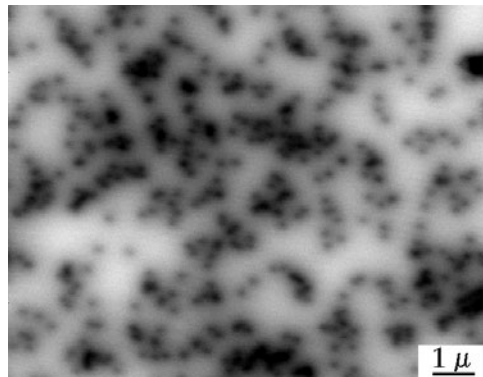


Figure 3. A typical EBIC image of a GaN epilayer obtained with $E_b = 35$ keV, $I_b = 3 \times 10^{-10}$ A.

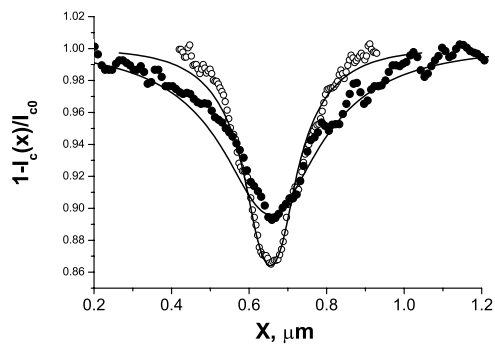


Figure 4. EBIC profiles of the threading dislocations in GaN with the average diffusion lengths $0.13 \mu\text{m}$ (open circles) and $0.3 \mu\text{m}$ (full circles). The curves simulated with $L_b = 0.15$ and $0.25 \mu\text{m}$ are shown by solid curves.

concerning the dislocation charge is very important for the correct calculation of dislocation recombination parameters from the EBIC contrast, because the dislocation charge not only increases the dislocation recombination strength but also drastically changes its dependence on the temperature and excitation level. Therefore, keeping in mind that the dislocations in GaN layers could be charged [8–13] and that due to the high carrier concentration and small lifetime the decrease of the dislocation barrier under e-beam excitation in GaN could be less substantial than in Si, the question concerning the effect of dislocation charge on the EBIC contrast is very important for this material.

3. Experimental study of dislocations in GaN

It is well established now, by EBIC and CL investigations [3–7], that dislocations in GaN enhance the excess carrier recombination. Their effect is strongly localized [3, 4, 6, 29], which could explain the relatively small effect of dislocations present in extremely high density on the optical device performance. In our studies the linear defects, the density of which correlates well with the dislocation density estimated from the x-ray diffractometry data and atomic force microscopy images, also produce a pronounced dark EBIC contrast (figure 3). It is seen that the width of the defect contrast is well below $1 \mu\text{m}$ even at large (35 keV) primary electron energy E_b . The profiles of such dislocations measured in the GaN structures with different

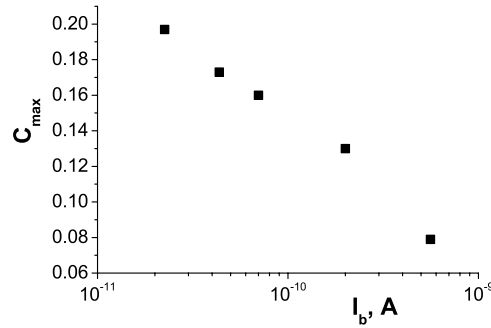


Figure 5. The dependence of the dislocation EBIC contrast for GaN on I_b measured at 300 K.

L_b are presented in figure 4. It is seen that the full width at half-maximum (FWHM) depends strongly on L_b .

The EBIC study of screw dislocations in n-type AlGaIn layers grown by plasma-induced molecular beam epitaxy [5] has shown that the contrast decreases with increasing temperature or with decreasing beam current I_b . Such behaviour was explained in the framework of the SRH model and under such assumptions the shallow acceptor level (20 meV above the valence band) was ascribed to dislocations. The opposite temperature dependence of the dislocation EBIC contrast in AlGaIn/GaN heterostructures grown by the same method was observed in [29]. And a pronounced decrease of the dislocation contrast with increasing I_b is observed in GaN grown by metal–organic chemical vapour deposition (MOCVD) (figure 5).

Thus, it could be concluded that dislocations in GaN are rather effective centres of nonradiative recombination. However, due to the small enough background diffusion length, the dislocation effect on the effective diffusion length is not so pronounced even at high dislocation densities. The studies of temperature and excitation level dependence of the dislocation recombination properties gave rather controversial results; this could be explained by the strong interaction of dislocations with impurities and/or intrinsic point defects. Some of the defects studied in different works could be not individual dislocations but dislocation–precipitate clusters; that also could explain the discrepancies observed. Such an explanation is confirmed by the large enough contrast value: exceeding 10% in [29] and in our experiments on MOCVD structures and reaching 80% in [5] (in the framework of the SRH model, 10% contrast corresponds to N_{tot} exceeding 10^8 cm^{-1} if a value of 10^{-14} cm^2 for σ was assumed). The contrast value reported in [5] leads to r_d exceeding 100 nm, which is too high for the clean individual dislocation. The high values of N_{tot} and r_d can also be understood by taking it into account that dislocations in GaN are charged. The EBIC contrast dependence on I_b seems to confirm the dislocation charge, because the beam currents used are too small for explaining the dependence presented in figure 5 in the framework of the SRH model. In this case, the SRH model cannot be applied and the more advanced models for the description of contrast dependence on temperature and/or excitation level should be used.

4. Simulation of the EBIC contrast of threading dislocations in GaN

The EBIC profiles of dislocations perpendicular to the surface in GaN were calculated using the procedure developed in [26, 27, 30]. The electron–hole pair generation function necessary for the calculations was obtained by Monte Carlo simulation and dislocations were described as cylinders with radius r_d and lifetime inside the cylinder τ_d . First of all, it should be noted

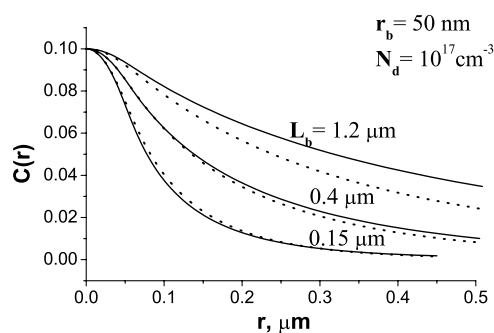


Figure 6. EBIC profiles of dislocations perpendicular to the surface simulated for $E_b = 20$ (dotted curves) and 35 keV (solid curves).

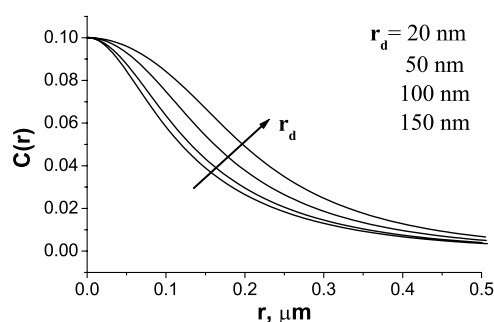


Figure 7. EBIC profiles of dislocations perpendicular to the surface simulated with $L_b = 0.2 \mu\text{m}$, $N_d = 10^{16} \text{cm}^{-3}$ and $E_b = 25 \text{keV}$.

that the main difference of the dislocation profile simulation for GaN from that for Si consists in the substantially smaller diffusion length in GaN, which is usually much smaller than R . Therefore, in contrast to the case for Si, the profile of the dislocation EBIC contrast in GaN depends mainly on the diffusion length but not on E_b (or R). Examples of dislocation contrast simulation are presented in figure 6 for $E_b = 20$ and 35 keV. It is seen that the FWHM does indeed strongly depend on L_b . It should also be noted that, while at large enough L_b the FWHM is smaller for smaller E_b , at small L_b the opposite relation holds.

To estimate the r_d -values, which could be extracted from the EBIC measurements, the dislocation contrast was simulated keeping constant $C_{max} = 10\%$ and changing r_d . The results obtained are presented in figure 7. It is seen that the profiles calculated with $r_d = 20$ and 50 nm show a noticeable difference that allows one to obtain the r_d -values down to 20 nm just from the profile of the dislocation EBIC contrast. The results of the simulation of the C_{max} -dependence on the applied bias are presented in figure 8. This method also allows one to obtain r_d as low as 20 nm and it seems to be less sensitive to the spatial variations of the background lifetime than the profile measurement. Thus, for materials with very low diffusion lengths, individual dislocations can be separated from dislocation clusters by profile measurements or by the study of the contrast dependence on the applied bias if the cluster dimensions exceed 20 nm.

5. Comparison of experimental and simulated results

The comparison of calculated dislocation EBIC profiles with those measured for the 3 μm thick GaN structures grown by MOCVD reveals a rather good correlation between them (figure 4).

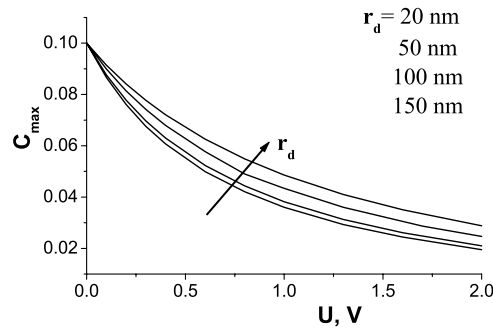


Figure 8. C_{max} -dependences on applied bias for dislocations perpendicular to the surface simulated with $N_d = 10^{16} \text{ cm}^{-3}$, $L_b = 0.2 \mu\text{m}$ and $E_b = 25 \text{ keV}$.

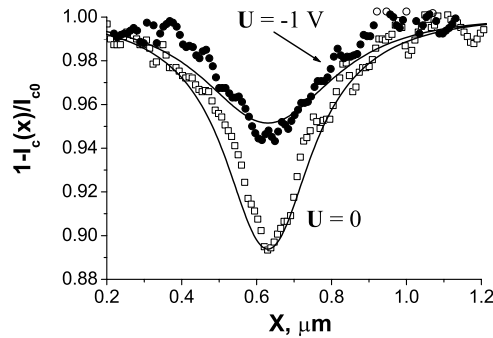


Figure 9. Dislocation EBIC profiles measured at $U = 0$ and -1 V . The profiles simulated with $r_d = 70 \text{ nm}$ are shown by the solid curves.

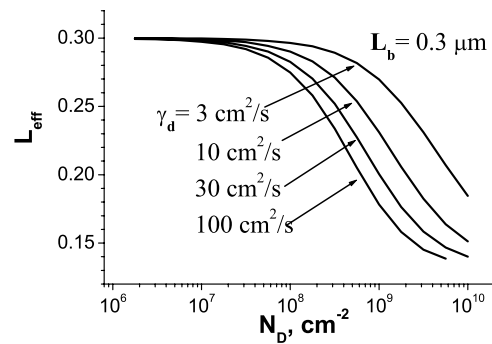


Figure 10. The calculated L_{eff} -dependence on the dislocation density N_D .

To fit the experimental profiles, the values of r_d , τ_d and L_b are varied. It should be mentioned that the L_b -values obtained by fitting the EBIC profiles were close to the average diffusion length values obtained from the I_c -dependence on E_b [31]. Thus, the bulk diffusion length in GaN can be estimated from the dislocation contrast profiles. The contrast dependence on applied bias also correlates rather well with the calculated profiles (figure 9).

The simulation carried out allows us to estimate the γ_d -value for individual threading dislocations, which is $20\text{--}30 \text{ cm}^2 \text{ s}^{-1}$. Using this value, the average diffusion length L_{eff}

as a function of dislocation density N_D could be estimated. The results of such estimations using the expression obtained in [32] under the assumption of negligible W are presented in figure 10. It is seen that, as expected, the dislocation effect is substantial only for distances between dislocations comparable with L_b . And from the similarity of the L_b - and L_{eff} -values, it follows that in the structures studied, L_b is smaller than the average distance between dislocations. Thus, it should be concluded that the low diffusion length in the GaN structures under study is mainly caused by other recombination centres and not by dislocations.

Acknowledgments

The author would like to thank Dr V V Sirotkin for kind provision of the programs used for the numerical simulation of the dislocation contrast, Professor S I Zaitsev for useful discussions concerning generation function calculations, Dr N M Shmidt, Dr A S Usikov and Dr E E Zavarin for kind provision of GaN structures for the EBIC investigations and O A Soltanovich for the C–V and DLTS measurements. This work was partially supported by the Russian National Scientific and Technology Programme ‘Physics of Solid State Nanostructures’.

References

- [1] Jain S C, Willander M and Narayan J 2000 *J. Appl. Phys.* **87** 96
- [2] Lester S S, Ponce F A, Craford M G and Steigerwald D A 1995 *Appl. Phys. Lett.* **66** 1249
- [3] Rosner S J *et al* 1997 *Appl. Phys. Lett.* **70** 420
- [4] Sugahara T *et al* 1998 *Japan. J. Appl. Phys.* **37** L398
- [5] Albrecht M *et al* 1999 *Phys. Status Solidi b* **216** 409
- [6] Cherns D, Henley S J and Ponce F A 2001 *Appl. Phys. Lett.* **78** 2691
- [7] Izumi T *et al* 2000 *J. Lumin.* **87–89** 1196
- [8] Look D C and Sizelove J R 1999 *Phys. Rev. Lett.* **82** 1237
- [9] Farvacque J-L, Bougrioua Z and Moerman I 2001 *Phys. Rev. B* **63** 115202
- [10] Youtsey C, Romano L T and Adesida I 1998 *Appl. Phys. Lett.* **73** 797
- [11] Hansen P J *et al* 1998 *Appl. Phys. Lett.* **72** 2247
- [12] Koley G and Spencer M G 2001 *Appl. Phys. Lett.* **78** 2873
- [13] Cherns D and Jiao C G 2001 *Phys. Rev. Lett.* **87** 205504
- [14] Im H-J *et al* 2001 *Phys. Rev. Lett.* **87** 106802
- [15] Elsner J *et al* 1998 *Phys. Rev. B* **58** 12571
- [16] Arslan I and Browning N D 2002 *Phys. Rev. B* **65** 075310
- [17] Wright A F and Grossner U 1998 *Appl. Phys. Lett.* **73** 2751
- [18] Lee S M *et al* 2000 *Phys. Rev. B* **61** 16033
- [19] Alexander H 1994 *Mater. Sci. Eng. B* **24** 1
- [20] Kittler M and Seifert W 1996 *Mater. Sci. Eng. B* **42** 8
- [21] Donolato C 1978/1979 *Optik* **52** 19
- [22] Donolato C 1992 *Semicond. Sci. Technol.* **7** 37
- [23] Wilshaw P R and Booker G R 1985 *Inst. Phys. Conf. Ser.* **76** 329
- [24] Kveder V, Kittler M and Schröter W 2001 *Phys. Rev. B* **63** 115208
- [25] Pasemann L 1991 *J. Appl. Phys.* **69** 6387
- [26] Sirotkin V V, Yakimov E B and Zaitsev S I 1996 *Mater. Sci. Eng. B* **42** 176
- [27] Sirotkin V V and Yakimov E B 1997 *Inst. Phys. Conf. Ser.* **160** 79
- [28] Shockley W and Read W T 1952 *Phys. Rev.* **87** 835
Hall R N 1952 *Phys. Rev.* **86** 600
- [29] Panin G N *et al* 1998 *Solid State Phenom.* **63–64** 131
- [30] Sirotkin V V and Yakimov E B 2001 *Solid State Phenom.* **78–79** 73
- [31] Shmidt N M *et al* 2002 *J. Phys.: Condens. Matter* **14**
- [32] Donolato C 1998 *J. Appl. Phys.* **84** 2656